of them very close to the active site. There is one negatively charged residue, Glu^{84}, about 12 Å away from the FTR disulfide, which fits with a positively charged residue in thioredoxin. The absence of charged groups, except for the one, makes the thioredoxin interaction area less specific, which might be important because FTR reduces different thioredoxins present in the cell, as is the case in the spinach chloroplast. Even *Synechocystis* FTR is capable of reducing spinach thioredoxin f. The ferredoxin interaction area, by contrast, is more specific owing to the presence of several charged residues. We observed a lower affinity between spinach ferredoxin and *Synechocystis* FTR (*5*) than was reported for the homologous couple spinach ferredoxin and FTR [M. Hirasawa *et al.*, *Biochim. Biophys. Acta* **935**, 1 (1988)].

13. S. Ciurli *et al.*, *J. Am. Chem. Soc.* **112**, 2654 (1990).
14. H. Laube, M. C. Kennedy, H. Beinert, C. D. Stout, *J. Mol. Biol.* **237**, 437 (1994).
15. M. Hirasawa *et al.*, *Biochemistry* **38**, 5200 (1999); Z. Salamon *et al.*, *Biochem. Biophys. Acta* **1230**, 114 (1995).
16. Z. Otwinowski and W. Minor, *Methods Enzymol.* **276**, 307 (1997).
17. D. Bailey, *Acta Crystallogr.* **D50**, 760 (1994).
18. E. de La Fortelle and G. Bricogne, *Macromol. Crystallogr.* **276**, 442 (1997).
19. Z. Otwinowski, in *Proceedings of the CCP4 Study Weekend*, W. Wolf, P. R. Evans, A. G. W. Leslie, Eds. (Science and Engineering Research Council, Daresbury Laboratory, Warrington, UK, 1991), pp. 80–88.
20. K. Cowtan, *Joint CCP4 ESF-EACBM Newslett. Protein Crystallogr.* **31**, 34 (1994).
21. T. A. Jones, J. Y. Zou, S. W. Cowan, M. Kjeldgaard, *Acta Crystallogr.* **47**, 110 (1991).
22. G. N. Murshudov, A. A. Vagin, E. J. Dodson, *Acta Crystallogr.* **D53**, 240 (1997).
23. V. S. Lamzin and K. S. Wilson, *Acta Crystallogr.* **D49**, 129 (1993).
24. R. A. Laskowski, M. W. MacArthur, D. S. Moss, J. M. Thornton, *J. Appl. Crystallogr.* **26**, 283 (1993).
25. B. L. Jacobson, Y. K. Chae, J. L. Markley, I. Rayment, H. M. Holden, *Biochemistry* **32**, 6788 (1993).
26. G. Capitani *et al.*, in (*5*), pp. 1939–1942.
27. K. Johansson *et al.*, *Biochemistry* **38**, 4319 (1999); P. D. Carr, D. Verger, A. R. Ashton, D. L. Ollis, *Structure* **7**, 461 (1999).
28. M. Chiadmi, A. Navazo, M. Miginac-Maslow, J.-P. Jacquot, J. Cherfils, *EMBO j.* **18**, 6809 (1999).
29. Supported by grants from the Swedish Council for Forestry and Agricultural Research and Swedish Natural Science Research Council (to H.E) and the Schweizerischer Nationalfonds (31-47107.96 to P.S.). Coordinates have been deposited in the Protein Data Bank (accession code 1dj7).

18 October 1999; accepted 7 December 1999

Voltage- and Tension-Dependent Lipid Mobility in the Outer Hair Cell Plasma Membrane

John S. Oghalai, Hong-Bo Zhao, J. Walter Kutz, William E. Brownell*

The mechanism responsible for electromotility of outer hair cells in the ear is unknown but is thought to reside within the plasma membrane. Lipid lateral diffusion in the outer hair cell plasma membrane is a sigmoidal function of transmembrane potential and bathing media osmolality. Cell depolarization or hyposmotic challenge shorten the cell and reduce membrane fluidity by half. Changing the membrane tension with amphipathic drugs results in similar reductions. These dynamic changes in membrane fluidity represent the modulation of membrane tension by lipid-protein interactions. The voltage dependence may be associated with the force-generating motors that contribute to the exquisite sensitivity of mammalian hearing.

Membranes define the boundaries of cells and maintain the electrochemical gradients required for life. In addition, the lateral wall plasma membrane of the mammalian cochlear outer hair cell (OHC) is involved in voltage-dependent changes in cell length, or electromotility (*1*). OHC electromotility is fundamental to the hearing sensitivity and selectivity of all mammals (*2*), but its mechanism is not known. Voltage-dependent changes in cell length must involve interactions between components of the plasma membrane and the cytoskeleton. We sought to investigate these lipid-protein interactions by measuring the fluidity of the phospholipid bilayer under three different experimental manipulations. We varied the membrane potential, modulated the intracellular pressure, and added drugs known to change membrane tension and curvature.

The rate of lateral diffusion of intramembrane lipids provides a measure of membrane fluidity (*3*). Lipid lateral diffusion can be affected by the phase state of the membrane, the individual types of membrane components (phospholipids, cholesterol, and protein), and their interactions (*4*). Guinea pig OHCs were isolated in vitro and stained with a fluorescent membrane lipid (di-8-ANEPPS) (*5*). We measured the lateral diffusion of di-8-ANEPPS in the lateral wall plasma membrane with fluorescence recovery after photobleaching (*6*). The diffusion coefficient of the lateral wall plasma membrane measured in this study ranged between 1.34×10^{-9} and 7.16×10^{-9} cm^2/s. These values are comparable to those previously reported for the OHC and lie within the range of those reported for other eukaryotic membranes (*5*, *7*).

OHC membrane potential was controlled by voltage clamp during measures of lateral diffusion (*8*). Membrane fluidity was voltage-dependent, decreasing up to 51% with depolarization (Fig. 1A). Saturation of the diffusion coefficient occurred at the voltage extremes. Sequential measurements of the diffusion coefficient in single cells at −60 mV, 0 mV, and then again at −60 mV revealed the voltage-dependent change in lateral diffusion to be reversible. The average diffusion coefficient went from $4.26 \times 10^{-9} \pm 0.42 \times 10^{-9}$ to $1.96 \times 10^{-9} \pm 0.33 \times 10^{-9}$ to $3.74 \times 10^{-9} \pm 0.55 \times 10^{-9}$ cm^2/s (mean ± SEM; $n = 4$). The diffusion coefficient in cultured rat hippocampal neurons (our control cells) did not change with changes in holding potential, going from $3.55 \times 10^{-9} \pm 0.24 \times 10^{-9}$ cm^2/s at −60 mV to $3.59 \times 10^{-9} \pm 0.21 \times 10^{-9}$ cm^2/s at 0 mV (mean ± SEM; $n = 9$).

Changes in membrane potential result in OHC length changes. Another way to change OHC length is to vary the intracellular pressure by changing the osmolality of the extracellular bathing media (*9*). Solutions with lower osmolality caused cell shortening and a decrease in the diffusion coefficient (Fig. 1, B and C). These effects were reversible, and both the cell length and the diffusion coefficient saturated at the osmotic extremes. The relation of cell length to membrane fluidity is exponential (Fig. 1D). Deiters' cells (supporting cells in the cochlea that co-isolate with OHCs) were used as controls. They underwent shape changes in response to osmotic challenge but had no change in their membrane diffusion coefficient.

Finally, the plasma membrane was directly manipulated by applying amphipathic drugs known to change membrane tension and curvature in red blood cells (RBCs) and COS cell cultures (*10*). The bilayer-couple hypothesis (*11*) argues that drugs which alter membrane curvature preferentially partition into either the outer or the inner leaflet of the phospholipid bilayer, selectively increasing that leaflet's surface area. Differences between outer and inner leaflet area alter membrane tension and curvature. We applied a drug that bends membranes outward (salicylate) and another that bends membranes inward (chlorpromazine) to a preparation containing guinea pig OHCs and RBCs (Fig. 2) (*12*). Although we found the expected morphologic changes in RBCs, the drugs evoked no change in the microscopic appearance of the OHCs ($n = 39$). However, measurements of OHC lipid lateral diffusion did show an effect of drug application (Fig. 2F). The presence of salicylate alone or chlorprom-

Department of Otolaryngology and Communicative Sciences, Baylor College of Medicine, One Baylor Plaza, Houston, TX 77030, USA.

*To whom correspondence should be addressed. E-mail: brownell@bcm.tmc.edu

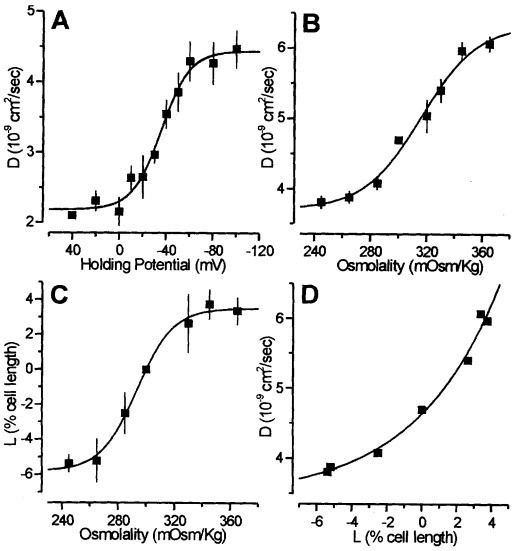

Fig. 1. Lateral diffusion in the OHC lateral wall plasma membrane. Each point is the average of at least five different measurements, each from a different cell. The error bars represent the SEM. (**A**) D was measured at holding potentials ranging from +40 to −100 mV (total of 70 measurements from 41 cells). The error bar for the point at 40 mV is smaller than the symbol size. The Boltzmann fit values are: $D_{depolarized} = 2.18 \times 10^{-9}$ cm^2/s, $D_{hyperpolarized} = 4.44 \times 10^{-9}$ cm^2/s, $V_{1/2} = -36$ mV, $s = 12$ mV (*23*). (**B**) D was measured while the osmolality of the extracellular solution was varied between 245 and 365 mOsm/kg (total of 275 cells, one measurement per cell). The error bar for the point at 300 mOsm/kg is smaller than the symbol size. The Boltzmann fit values are: $D_{hypotonic} = 3.70 \times 10^{-9}$ cm^2/s, $D_{hypertonic} = 6.34 \times 10^{-9}$ cm^2/s, $Osm_{1/2}$ (the osmolality at the midpoint of the change in D) = 316 mOsm/kg, $s = 20$ mOsm/kg. The slightly higher D values in these cells compared with those in (A) may be related to differences in intracellular pressure associated with the patch-clamp technique (*17*). (**C**) The percent change in cell length (L) was measured while the osmolality of the extracellular solution was varied. This was normalized to their length at 300 mOsm/kg (total of 154 measurements from 77 cells). The Boltzmann fit values are: $L_{hypotonic} = -5.79\%$, $L_{hypertonic} = 3.51\%$, $Osm_{1/2} = 294$ mOsm/kg, $s = 13$ mOsm/kg. (**D**) D was plotted versus L [with the same data as (B) and (C)]. The relation was fit with an exponential function, $D = D_0 + A\exp(RL)$, with fit values $D_0 = 3.43 \times 10^{-9}$ cm^2/s, $A = 1.21 \times 10^{-9}$ cm^2/s, $R = 0.21$.

azine alone reduced the diffusion coefficient by 53 and 33%, respectively. There was no significant difference between the diffusion coefficient of control OHCs and OHCs incubated in salicylate and chlorpromazine together. Perfusion of the curvature-altering drugs did not change the zero-current potentials or current-voltage characteristics of OHCs under voltage clamp (*13*). We measured the electromotile voltage-displacement relations with a voltage-step protocol (Fig. 3) (*14*). OHCs bathed in either the control medium or in chlorpromazine alone had similar transfer functions. OHCs bathed in salicylate alone had an attenuated electromotile response. Although chlorpromazine had reversed salicylate's effect on lateral diffusion, it did not reverse salicylate's attenuation of electromotility.

Here the dynamic modulation of membrane fluidity is described. Specifically, we measured the lateral diffusion of a fluorescent probe as an estimate of lipid (as opposed to protein) mobility within the plasma membrane. The voltage range over which lateral diffusion is voltage-dependent suggests that the change in membrane fluidity is linked to electromotility. Our measurements are sensitive to the lipid-protein interactions that occur in the membrane, and the shape of the voltage-diffusion coefficient relation extends our understanding of the interaction between the motor complex and the plasma membrane. An intramembrane area–motor that flickers between two states (*15*) should agitate the surrounding membrane phospholipids and result in an increased lateral diffusion. Because the highest rate of flicker should occur at the $V_{1/2}$ (the potential at the midpoint of the length change) of the electromotility transfer function (*16*), the diffusion coefficient would be expected to peak between −40 and −20 mV. Our data do not reveal a peak in this voltage range. However, electromotility and membrane tension are intimately related. Tension applied to the OHC influences the voltage dependence of electromotility and modulates the nonlinear capacitance of the plasma membrane (*15*, *17*, *18*). It is likely that changes in membrane tension, induced by each of our experimental manipulations, are responsible for the dynamic changes in membrane fluidity.

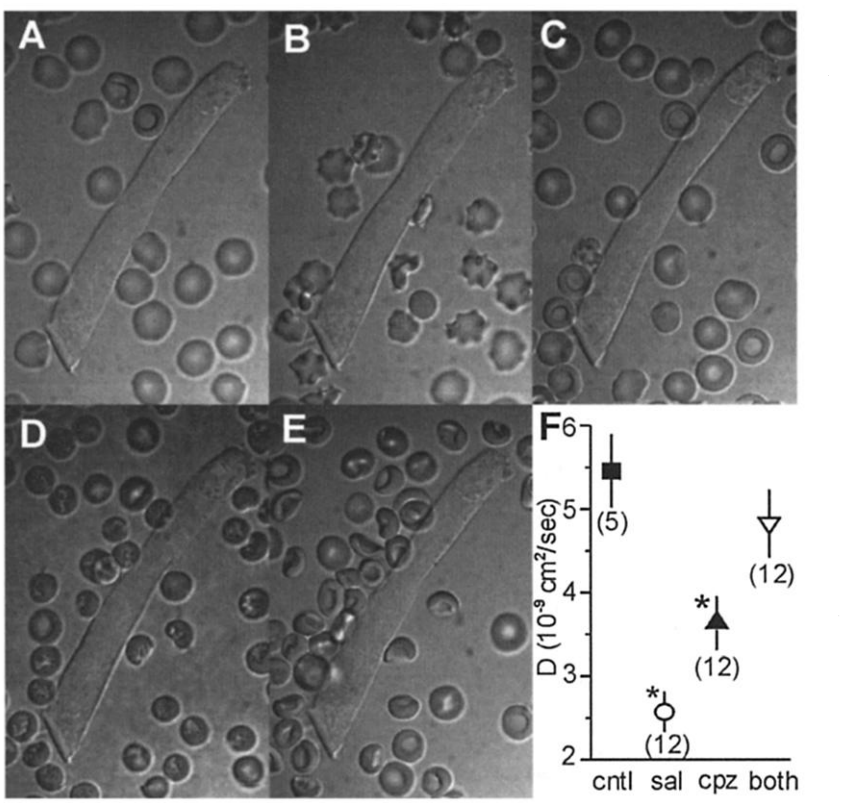

Fig. 2. The effects of curvature-altering drugs on cell morphology and lateral diffusion. The RBCs serve as a bioassay for the curvature-altering drugs. (**A**) RBCs were biconcave in the control solution, (**B**) crenulated in salicylate alone, (**C**) biconcave in a solution of salicylate and chlorpromazine combined, (**D**) cupped in chlorpromazine alone, and (**E**) biconcave after wash-out with control solution. During this 5-min sequential drug application, the length, width, and morphologic appearance of the OHC did not change appreciably. (**F**) The D value of the OHC lateral wall plasma membrane was reduced from controls (cntl) in the presence of either salicylate alone (sal) or chlorpromazine alone (cpz). It was unchanged in the presence of salicylate and chlorpromazine combined (both) ($P = 0.38$). The values in parentheses indicate the number of cells averaged together for each measurement and the error bars represent the SEM; a significant difference from control is indicated by an asterisk ($P < 0.01$, Student's nonpaired t-test). The D values were as follows (mean ± SEM): cntl, $5.46 \times 10^{-9} \pm 0.44 \times 10^{-9}$ cm^2/s; sal, $2.58 \times 10^{-9} \pm 0.25 \times 10^{-9}$ cm^2/s; cpz, $3.64 \times 10^{-9} \pm 0.32 \times 10^{-9}$ cm^2/s; both, $4.83 \times 10^{-9} \pm 0.41 \times 10^{-9}$ cm^2/s.

Most membranes bend easily, as seen by changes in membrane curvature driven by thermal fluctuations (*19*). Microscopic changes in RBC membrane curvature with amphipathic drug application are evident as crenulation or cupping. However, none of our manipulations generated visible bending of the OHC plasma membrane. This may reflect the fact that the stiffness parameter of the OHC is much greater than that of the RBC (*20*). Despite the lack of evidence for microscopic changes in OHC membrane curvature, the highly organized, orthotropic nature of the OHC cytoskeleton could permit nanoscale changes in membrane curvature (Fig. 4). As the OHC shortens, the inter-actin distance would decrease and result in increased membrane crenulations. The bending associated with the interactions between the cytoskeleton and the plasma membrane modulates membrane tension.

The maximal size of the crenulations when the OHC is depolarized can be estimated by assuming the membrane to be flat when the OHC is hyperpolarized. Assuming a maximum cell shortening of 7.5%, the inter-actin distance would decrease from 40 to 37 nm; however, the intervening membrane would still be 40 nm long. Modeling this as two back-to-back right triangles, each base would be 18.5 nm and each hypotenuse would be 20 nm. The angle between the base and the hypotenuse is >20° and the crenulation height is 7.6 nm (slightly greater than the width of most biological membranes). The nanoscale membrane rippling in the shortened cell means there is ~10% greater membrane surface area than the cell's apparent surface area under the microscope. This, however, could not account for the 50% change in the diffusion coefficient we measured. Transmission electron microscopy of the OHC consistently reveals submicroscopic crenulations in the lateral wall plasma membrane (*21*). Although this is most likely due to fixative-induced shrinkage of the proteins of the cytoskeleton and it demonstrates that the membrane will bend with the cytoskeleton, there is no evidence that the actin-spectrin network is the active element in electromotility.

Our data indicate that OHC membrane tension can be modulated by voltage, osmotic challenge, and curvature-inducing drugs. Changes in tension, in turn, appear to affect the molecular environment of the membrane, changing its fluidity. This is compatible with a model of passive nanoscale changes in membrane curvature, which could be based on an area-motor mechanism in which the lipid-protein interactions generate progressive changes in membrane tension. Alternative possibilities for the electrically evoked changes include an interaction of the probe with the glycocalyx of the cell or a variation in the binding properties of the probe; however, the osmotic results and our control experiments suggest such possibilities are unlikely. Four voltage-dependent phenomena have been identified with the lateral wall over the past 15 years. Voltage-dependent length changes (*1*), cell stiffness (*22*), and lateral diffusion are unique to the OHC. Nonlinear membrane capacitance (*16*) shows that a membrane-bound charge movement is associated with electromotility, possibly within the motor complex itself. A complete understanding of electromotility must explain all four phenomena and will undoubtedly provide an explanation for the elegant organization of the lateral wall.

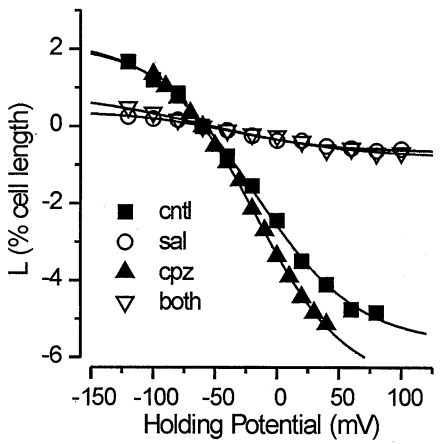

Fig. 3. The effects of curvature-altering drugs on OHC electromotility. The percent change in cell length (*L*) was measured as the holding potential was varied, normalized to cell length at −60 mV. The control cell (cntl) demonstrated the normal electromotile response. The presence of chlorpromazine alone (cpz) did not suppress electromotility. Salicylate alone (sal) blunted the electromotile response. Chlorpromazine failed to restore electromotility in the presence of salicylate (both). Each curve was obtained from a different cell. The Boltzmann fit values are: cntl, $L_{hyperpolarized} = 2.25\%$, $L_{depolarized} = -5.64\%$, $V_{1/2} = -19$ mV, $s = 42$ mV; sal, $L_{hyperpolarized} = 0.39\%$, $L_{depolarized} = -0.65\%$, $V_{1/2} = -35$ mV, $s = 41$ mV; cpz, $L_{hyperpolarized} = 2.10\%$, $L_{depolarized} = -6.73\%$, $V_{1/2} = -17$ mV, $s = 37$ mV; both, $L_{hyperpolarized} = 0.91\%$, $L_{depolarized} = -0.81\%$, $V_{1/2} = -58$ mV, $s = 59$ mV.

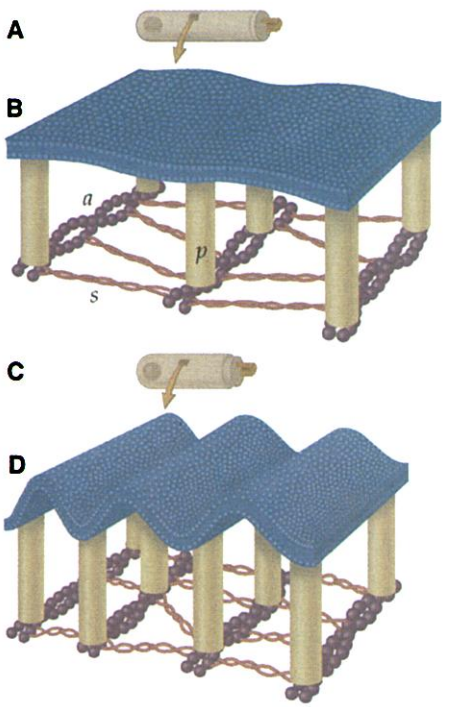

Fig. 4. Hypothetical nanoscale membrane rippling within the lateral wall of the OHC. The plasma membrane is tethered to a subplasmalemmal cytoskeleton by 30-nm-long "pillars" (*p*) (*24*). The molecular composition of the pillars is unknown. The pillars bond to parallel actin filaments (*a*) that run circumferentially around the cell. The actin filaments are spaced about 40 nm apart and cross-linked with molecules of spectrin (*s*) that run longitudinally along the cell. (**A** and **C**) The OHC when hyperpolarized and depolarized, respectively. Depolarization makes the OHC shorter and wider. (**B** and **D**) Potential alterations in membrane curvature resulting from electromotile length changes. Note the increased membrane crenulations in (D).

References and Notes

1. W. E. Brownell, C. R. Bader, D. Bertrand, Y. de Ribaupierre, *Science* **227**, 194 (1985).
2. P. Dallos, *J. Neurosci.* **12**, 4575 (1992); J. S. Oghalai *et al.*, *J. Neurophysiol.* **79**, 2235 (1998); H.-B. Zhao and J. Santos-Sacchi, *Nature* **399**, 359 (1999).
3. W. L. C. Vaz, Z. I. Derzko, K. A. Jacobson, in *Membrane Reconstitution*, G. Poste and G. L. Nicolson, Eds. (Elsevier, Amsterdam, 1982) pp. 83–136.
4. D. E. Golan, M. R. Alecio, W. R. Veatch, R. R. Rando, *Biochemistry* **23**, 332 (1984).
5. The organ of Corti was isolated from the cochleae of guinea pigs, incubated for 3 to 5 min with trypsin, and dissociated onto a microwell petri dish. For some experiments, rat hippocampal neurons were used as a control. These cells were harvested on embryonic day 19 and grown in culture for 9 to 12 days in serum-free medium. Dissection and experiments were performed at 22°C in an extracellular solution consisting of the following: 155 mM NaCl, 4 mM KCl, 1 mM $MgCl_2$, 2 mM $CaCl_2$, 10 mM Hepes, and 10 mM glucose. The solution was adjusted to a pH of 7.3 and an osmolality of 320 mOsm/kg. We stained the plasma membrane of the isolated cells with di-8-ANEPPS, a fluorescent molecule with a short hydrophobic tail that inserts itself into the outer leaflet of the phospholipid bilayer. Di-8-ANEPPS (75 μM) was dispersed into extracellular solution by sonication for 1 min, and the cells were stained for 5 min before unbound dye was thoroughly rinsed away with extracellular solution alone [V. Montana, D. L. Farkas, L. M. Loew, *Biochemistry* **28**, 4536 (1989); J. S. Oghalai, T. D. Tran, R. M. Raphael, T. Nakagawa, W. E. Brownell, *Hear. Res.* **135**, 19 (1999)].
6. Imaging was performed using a Bio-Rad (Hercules, CA) scanning confocal system with a krypton/argon laser, configured on an Axiovert 35 microscope (Carl Zeiss, Jena, Germany) with a 100× oil immersion objective. The laser excitation wavelength was 488 nm; the fluorescent emission was collected using a long-pass filter with a corner wavelength of 515 nm. We initially positioned the laser beam of the confocal microscope tangential to the OHC lateral wall to create a photobleached spot. The laser power was 50 μW and the spot radius was roughly 5 μm. Rapid scanning confocal images were then taken over the next minute to document the recovery phase. The three-point fit method was used to determine the membrane diffusion coefficient. For the drug application experiments, only a single diffusion coefficient measurement was made per cell. For the voltage-clamp experiments, up to four measurements of the diffusion coefficient were made per OHC. Each measurement was made at a different location along the lateral wall. Due to difficulties with phototoxicity, it

was impossible to collect a large number of data points from a single cell. We stopped using a cell when a change in the input impedance indicated either membrane breakdown or a loss of the tight seal between the recording pipette and the cell membrane. Most cells allowed one to three measurements [D. Axelrod, D. E. Koppel, J. Schlessinger, E. Elson, W. W. Webb, *Biophys. J.* **16**, 1055 (1976)].
7. Z. Derzko and K. Jacobson, *Biochemistry* **19**, 6050 (1980); N. L. Thompson and D. Axelrod, *Biochim. Biophys. Acta* **597**, 155 (1980); H. G. Kapitza and E. Sackmann, *Biochim. Biophys. Acta* **595**, 56 (1980); J. A. Bloom and W. W. Webb, *Biophys. J.* **42**, 295 (1983).
8. Whole-cell patch clamping was performed with a patch pipette intracellular solution consisting of the following: 150 mM KCl, 5 mM $MgCl_2$, 5 mM EGTA, and 10 mM Hepes, with an osmolality of 305 mOsm/kg and a pH of 7.3. Gigohm seals were formed at the base of the OHCs. After the whole-cell mode was entered, the series resistance was between 10 and 30 megohms. On-line series resistance compensation was 75 to 95%, and residual series resistance was not compensated.
9. Osmotic challenge experiments were performed using a lower NaCl concentration (130 mM). Glucose was added as needed to achieve osmolalities from 265 to 365 mOsm/kg. A 245 mOsm/kg solution was created by adding additional free water.
10. B. Deuticke, *Biochim. Biophys. Acta* **163**, 494 (1968); M. P. Sheetz, R. G. Painter, S. J. Singer, *J. Cell Biol.* **70**, 193 (1976); A. J. Patel *et al.*, *EMBO J.* **17**, 4283 (1998).
11. M. P. Sheetz and S. J. Singer, *Proc. Natl. Acad. Sci. U.S.A.* **71**, 4457 (1974); *J. Cell Biol.* **70**, 247 (1976).
12. Sodium salicylate (10 mM) and/or chlorpromazine (0.1 mM) were included in the extracellular solution for these experiments. These concentrations were chosen because they cause equal and opposite membrane bending in the RBC (*10, 11*). All solutions were adjusted to a pH of 7.3 and an osmolality of 320 mOsm/kg.
13. W. E. Shehata, W. E. Brownell, R. Dieler, *Acta Oto-Laryngol.* **111**, 707 (1991).
14. Images of outer hair cell electromotility were recorded on Super-VHS videotape. Length measurements were made off-line with NIH Image software. The apical edge of the cell was determined by fitting the pixel intensity function with a parabola and using the local maximum as the border.
15. K. H. Iwasa, *Biophys. J.* **65**, 492 (1993); *J. Acoust. Soc. Am.* **96**, 2216 (1994); P. Dallos, B. N. Evans, R. Hallworth, *Nature* **350**, 155 (1991).
16. J. Santos-Sacchi, *J. Neurosci.* **11**, 3096 (1991); G. Huang and J. Santos-Sacchi, *Proc. Natl. Acad. Sci. U.S.A.* **91**, 12268 (1994); J. E. Gale and J. F. Ashmore, *Nature* **389**, 63 (1997).
17. S. Kakehata and J. Santos-Sacchi, *Biophys. J.* **68**, 2190 (1995); K. H. Iwasa and R. S. Chadwick, *J. Acoust. Soc. Am.* **92**, 3169 (1992).
18. J. E. Gale and J. F. Ashmore, *Proc. R. Soc. London Ser. B* **255**, 243 (1994); M. Adachi and K. H. Iwasa, *Proc. Natl. Acad. Sci. U.S.A.* **96**, 7244 (1999).
19. R. M. Servuss, W. Harbich, W. Helfrich, *Biochim. Biophys. Acta* **436**, 900 (1976); M. Bloom, E. A. Evans, O. Mouritsen, *Q. Rev. Biophys.* **24**, 293 (1991).
20. P. S. Sit, A. A. Spector, A. Lue, A. S. Popel, W. E. Brownell, *Biophys. J.* **72**, 2812 (1997); J. S. Oghalai, A. A. Patel, T. Nakagawa, W. E. Brownell, *J. Neurosci.* **18**, 48 (1998).
21. C. A. Smith, *Ann. Otol. Rhinol. Laryngol.* **77**, 629 (1968).
22. D. Z. He and P. Dallos, *Proc. Natl. Acad. Sci. U.S.A.* **96**, 8223 (1999).
23. The data were fit with a Boltzmann function, $D = D_{depolarized} + (D_{hyperpolarized} - D_{depolarized})/\{1 + \exp[(V - V_{1/2})/s]\}$, where D is the diffusion coefficient at the membrane potential V, $D_{hyperpolarized}$ and $D_{depolarized}$ are the diffusion coefficients at the hyperpolarized and depolarized states, $V_{1/2}$ is the potential at the midpoint of the change in D, and s describes the voltage dependency of the curve (slope factor). The data were fit by computer algorithm.
24. M. J. Holley, in *The Cochlea*, P. Dallos, A. N. Popper, R. R. Fay, Eds. (Springer, New York, 1996), vol. 8, pp. 386–434.
25. All procedures were approved by the animal care and use committee at the Baylor College of Medicine. Supported by the Jake and Nina Kamin Chair and by research grants from the Deafness Research Foundation (J.S.O.) and NIDCD (W.E.B.). J.S.O. developed the techniques for measuring lateral diffusion used in this manuscript and collected the data for Figs. 1A, 2, and 3. H.-B.Z. and J.W.K. collected the data for Fig. 1, B, C, and D. We thank B. R. Alford, A. Bullen, R. A. Eatock, H. A. Jenkins, T. Nakagawa, A. Nygren, A. S. Popel, R. M. Raphael, F. Sachs, P. Saggau, A. A. Spector, and T. D. Tran.

8 October 1999; accepted 2 December 1999

Creating a Protein-Based Element of Inheritance

Liming Li and Susan Lindquist*

Proteins capable of self-perpetuating changes in conformation and function (known as prions) can serve as genetic elements. To test whether novel prions could be created by recombinant methods, a yeast prion determinant was fused to the rat glucocorticoid receptor. The fusion protein existed in different heritable functional states, switched between states at a low spontaneous rate, and could be induced to switch by experimental manipulations. The complete change in phenotype achieved by transferring a prion determinant from one protein to another confirms the protein-only nature of prion inheritance and establishes a mechanism for engineering heritable changes in phenotype that should be broadly applicable.

Two genetic elements in *Saccharomyces cerevisiae*, [*PSI*$^+$] and [*URE3*], are widely believed to transmit phenotypes through proteins with self-perpetuating changes in conformation, rather than through altered nucleic acids (*1*). These elements are called yeast prions because of conceptual similarities between their modes of transmission and that postulated for the infectious agent in mammalian prion diseases (*2*). The yeast proteins, however, are unrelated to the mammalian prion protein and to each other. Moreover, they usually do not kill the organism, but produce cytoplasmically transmitted, heritable changes in phenotype (*3, 4*). For [*PSI*$^+$], the protein determinant is Sup35, a translation termination factor. In [*psi*$^-$] cells, Sup35 is soluble and functional (*5, 6*). In [*PSI*$^+$] cells, most Sup35 is insoluble and nonfunctional, causing a change in translation fidelity (*5, 6*). This phenotype is heritable because Sup35 protein in the [*PSI*$^+$] state influences new Sup35 protein to adopt the same state and passes from mother cell to daughter to perpetuate the cycle of conversion (*6–8*). [*PSI*$^+$] is, however, metastable: [*PSI*$^+$] cells occasionally give rise to [*psi*$^-$] cells and vice versa (*3*), as the [*PSI*$^+$] conformation is lost or gained.

Sup35 has three distinct regions (*9*). The NH_2-terminus (N) plays a critical role in Sup35's self-perpetuating change in state (*10–13*). The middle region (M) provides a solubilizing and/or spacing function (*14*). The COOH-terminus (C) provides translation-termination activity (*10, 15*). To test whether other proteins can be made to undergo a prion-like change in state, we fused N and M to a steroid hormone–regulated transcription factor, the rat glucocorticoid receptor (GR), and to a constitutive variant (GR^{526}) (*16*) that lacks the heat shock protein 90 (Hsp90) and hormone-binding domain (Fig. 1A) (*17*). The fusion did not block GR's inherent transcriptional activity: when NMGR and GR were expressed in [*psi*$^-$] cells over a broad range of induction levels, the activity of NMGR was in each case similar to that of GR (Fig. 1B, left). NMGR^{526} and GR^{526} also had similar activities in [*psi*$^-$] cells (*18*).

Three lines of evidence indicate that NM fusion proteins can interact with endogenous Sup35 to undergo prion-like changes in state. First, in contrast with [*psi*$^-$] cells, in [*PSI*$^+$] cells, newly synthesized NMGR had much lower activity than GR (Fig. 1B, right). Immunoblotting demonstrated that this was not due to a reduction in NMGR expression (*18*). Second, transient expression of NMGR, but not of GR, induced new heritable [*PSI*$^+$] elements in [*psi*$^-$] cells (Table 1). The NMGR^{526} variant also induced [*PSI*$^+$] elements, but not if the protein carried a small deletion of residues 22 through 69 in N (Δ22–69) (Table 1), which blocks [*PSI*$^+$] induction by Sup35 (*10*). Third, NMGR and NMGR^{526} exhibited the same unusual pattern of plasmid incompatibility as Sup35 (*10, 13*). High-copy Sup35 plasmids cannot be transformed into [*PSI*$^+$] cells because excessive Sup35 aggregation inhibits translational termination so severely that cells die. Cells are immune to the toxicity of the plasmid when the genomic copy of *SUP35* has its N and M regions deleted (Δ*NMSUP35*) (*10, 13*). Conversely, plasmids are not toxic if they carry the Δ22–69 deletion. When GR and NMGR were

Howard Hughes Medical Institute, Department of Molecular Genetics and Cell Biology, University of Chicago, 5841 South Maryland Avenue MC1028, Chicago, IL 60637, USA.

*To whom correspondence should be addressed. E-mail: S-Lindquist@uchicago.edu